

# Ultrasound Speckle Detection Using Low Order Moments

Hassan Rivaz  
 Department of Computer Science  
 Johns Hopkins university  
 Baltimore, MD, 21218  
 Email: rivaz@jhu.edu

Emad M. Boctor  
 Department of Computer Science  
 Johns Hopkins University  
 Baltimore, MD, 21218  
 Email: eboctor@cs.jhu.edu

Gabor Fichtinger  
 Department of Computer Science  
 Johns Hopkins university  
 Baltimore, MD, 21218  
 Email: gaborf@jhu.edu

**Abstract**—Speckle detection is essential in many areas of quantitative ultrasound. In this work, speckle is characterized with  $R$ =SNR and  $S$ =skewness of the amplitude of the ultrasound signal data  $A$ . Different powers of  $A$  can be used to calculate  $R$  and  $S$ . Prager et al. [1] proposed a method for finding the optimum power value, which then was further scrutinized [2]. We propose using two different powers of  $A$  in  $R$  and  $S$ , and perform a large number of computer simulations to find these optimal values.

## I. INTRODUCTION

Each pixel in an ultrasound image is formed by the back scattered echoes from an approximately ellipsoid called the resolution cell (Figure 1). The interference of scatterers in a resolution cell creates the granular appearance of the ultrasound image, called speckle. Although of random appearance, speckle pattern is identical if the same object is scanned from the same direction and under the same focusing and frequency.

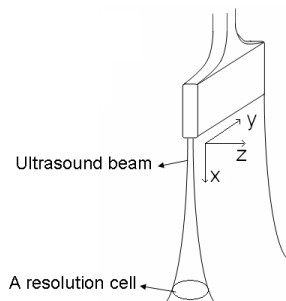


Fig. 1. Ultrasound beam is in order of a millimeter wide. This wideness affects the resolution of ultrasound image, as well as creating a granular pattern, called speckle. The diameter of the ellipsoid in the axial direction (x axis) is magnified in this image.

Diffuse scattering happens if the scatterers in a resolution cell are placed independently and uniformly at random. If each resolution cell in an image patch has many such scatterers, the patch is said to be fully developed speckle (FDS). In contrast, white and dark features in the ultrasound B-mode images are caused by coherent back-scattering of ultrasound pulse.

Speckle detection is useful in segmentation, sensorless 3D freehand US, speckle cancellation and quantitative tissue

characterization. In ultrasound compounding, for example, the goal is to cancel the speckles, while in sensorless 3D freehand ultrasound they are utilized to estimate probe movement.

Assume the effective number of scatterers per resolution cell to be  $\mu$ , and the diffuse and coherent signal energy to be  $2\sigma^2$  and  $s^2$  respectively. Speckles can be classified by  $\mu$  and  $k = \frac{s}{\sigma}$ , with  $\mu > 10$  and  $k < 1$  being FDS.

Dutt et al. [3], [4] and Prager et al. [1] proposed using  $R$  and  $S$  to estimate  $\mu$  and  $k$  and therefore classify speckles

$$R = \text{SNR} = \frac{\langle A^v \rangle}{\sqrt{\langle A^{2v} \rangle - \langle A^v \rangle^2}} \quad (1)$$

$$S = \text{skewness} = \frac{\langle (A^v - \langle A^v \rangle)^3 \rangle}{(\langle A^{2v} \rangle - \langle A^v \rangle^2)^{\frac{3}{2}}} \quad (2)$$

where  $A$  is the amplitude of the ultrasound RF envelope,  $v$  is the signal power and  $\langle \dots \rangle$  denotes mean. Depending on the correlation of data, thousands of sample data are required to reliably calculate  $R$  and  $S$  [4]. In [4] and [1], values of  $v$  that reduce this sample size are sought. Useful variability of clusters of sample data with different  $\mu$  and  $k$  values are maximized in [1] to find the optimal  $v$ , a method that is scrutinized by [2].

Since  $R$  and  $S$  are different order moments of sample data, optimal values for  $v$  in  $R$  and  $S$  are not necessarily the same. We propose using different values of  $v$  in  $R$  and  $S$ . We follow a similar approach to [1] to simulate the B-scan.

## II. SIMULATION METHODS

We seek the optimal values of  $v_R$  and  $v_S$  that substitute  $v$  in equations 1 and 2 respectively. To create the sample data, the sum of  $\mu$  vectors of length  $\sqrt{2/\mu}$  and arbitrary phase (a random walk) is added to a single vector with zero phase and length  $k$ , resulting in a vector  $\mathbf{A}$ , with amplitude  $A$ .

The first step to compare the performance of different values for  $v_R$  and  $v_S$  is to obtain an FDS discriminant function. To this end, we set  $v_R = 0.2, 0.4 \dots 3$  and similarly  $v_S = 0.2, 0.4 \dots 3$ , and for all combinations of  $v_R$  and  $v_S$  ( $15 \times 15 = 225$  cases) acquire an FDS elliptical discrimination function in 3 steps (Figure 2):

- 1) 30000 sets of 5000 random  $A$  that represent FDS with different parameters  $0 < k < 1$  and  $10 < \mu < 60$  are

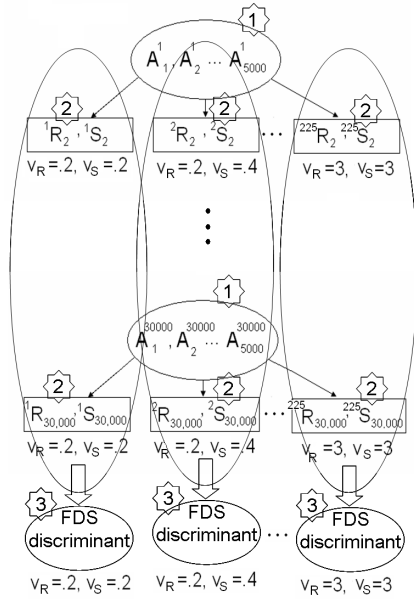


Fig. 2. The procedure for acquiring the elliptical discriminant function for all values of  $0 < v_R < 3$  and  $0 < v_S < 3$ . Each data sample  $A$  is calculated by a random walk described above, not shown in Figure 2).  
 2) For each set,  $R$  and  $S$  are calculated for all combinations of  $0.2 \leq v_S \leq 3$  and  $0.2 \leq v_R \leq 3$ , resulting in  $30000 \times 225$  samples of  $R$  and  $S$ .  
 3) Using the 30000 samples of  $R$  and  $S$  for each  $v_R$  and  $v_S$  combination, 225 elliptical discriminant functions that encompass 95% of  $R$  and  $S$  values is obtained automatically using PCA and the covariance method.

Figure 3 shows the elliptical discriminant functions for  $v_R = 0.2$  and  $v_S = 0.2$  in the left images and for  $v_R = 2$  and  $v_S = 0.8$  in the right ones. The two top images show 100  $(R, S)$  points that correspond to 100 sets of data  $A$  with  $\mu = 6$  and  $k = 0$  values (few scatterers). These sets have to be categorized as non-FDS, therefore one can say that the pair  $v_R = 2$  and  $v_S = 0.8$  is performing better in this case (minimizing false acceptance). In the two bottom images, same  $v_R$  and  $v_S$  values are used, but for  $\mu = 12$  and  $k = 0$  (many scatterers, FDS). Both left and right discriminant functions categorize all 100 sets correctly (minimizing false rejection). This example shows that different  $v_R$  and  $v_S$  values affect the performance of the discriminant function.

In order to find the optimal  $v_R$  and  $v_S$  values, we obtain the probability that a set with properties  $\mu$  and  $k$  be identified as FDS, i.e. the  $(R, S)$  pair calculated for this set falls inside the ellipse. Having such a pseudo pdf ( $p_{FDS}$ ) for all values

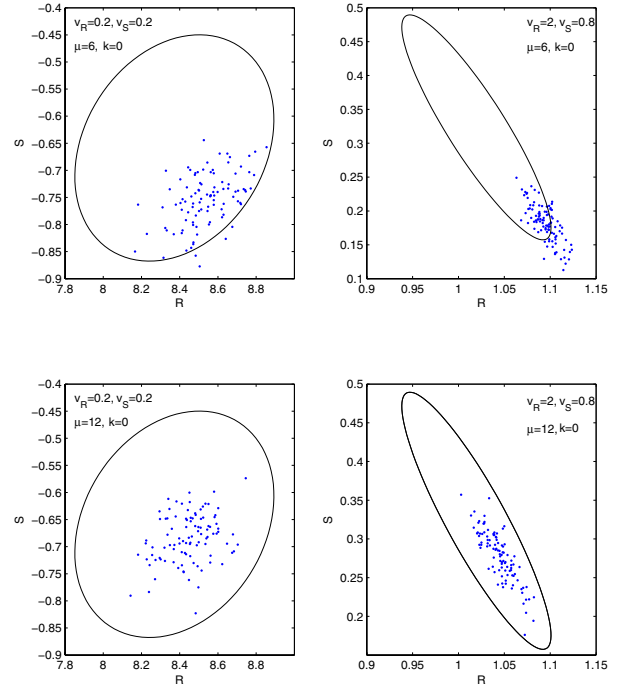


Fig. 3. The elliptical discriminant function and 100 points corresponding to 100 sets with different  $v_R$  and  $v_S$  values as labelled (each set has 5000 sample data  $A$ ). In the two top figures, the sets are not FDS, since they have few scatterers. Therefore, ideally they all have to be placed outside the elliptical discriminant function. The two bottom figures the sets are FDS and the ellipse is expected to encompass them.

of  $\mu$ ,  $k$ ,  $v_R$  and  $v_S$ , it is possible to optimize  $v_R$  and  $v_S$  to achieve a desired probability distribution. Obtaining  $p_{FDS}$ , which requires a large number of simulations, is as follows.

- 1) For all combinations of  $k = 0, 0.1, 0.2 \dots 1.5$  (16 values) and  $\mu = 2, 3 \dots 60$  (59 values) in the  $k - \mu$  plane (Figure 4), generate 100 sets of 5000 random  $A$ . The result is  $16 \times 59 \times 100 \times 5000$  random  $A$ , with each  $A$  being calculated by a random walk.
- 2) Calculate  $R$  and  $S$  of each set for all combinations of  $v_R$  and  $v_S$ .
- 3)  $p_{FDS}$  = number of the  $(R, S)$  pairs that fall inside the FDS discriminant ellipse. The resultant  $p_{FDS}$  is a function of  $v_R$ ,  $v_S$ ,  $\mu$  and  $k$ .

Different optimum values for  $v_R$  and  $v_S$  can be found depending on the criteria.

### III. OPTIMIZING $v_R$ AND $v_S$

Using  $p_{FDS}$  and depending on the particular application, different optimum values for  $v_R$  and  $v_S$  can be found. We analyze three cases here.

#### A. Minimizing False Acceptance for Coherent Sets

To minimize false acceptance for the coherent data, one can sum  $p_{FDS}$  over the area  $C$  in Figure 4. Figure 5 top

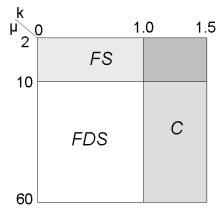


Fig. 4. The regions with  $\mu < 10$  and  $k > 1$  are labelled by *FS* (few scatterers) and *C* (coherent) respectively.

left shows the summation result. Generally speaking, the four corners of the  $v_R - v_S$  plane should be avoided to prevent false acceptance. The *FDS* discriminant ellipse along with  $(R, S)$  of 100 sets of 5000 sample *A* for three values of  $v_R = 0.4, v_S = 0.2, v_R = 3, v_S = 3$  (bad choices) and  $v_R = 1.2, v_S = 0.6$  (good choice) are also shown.

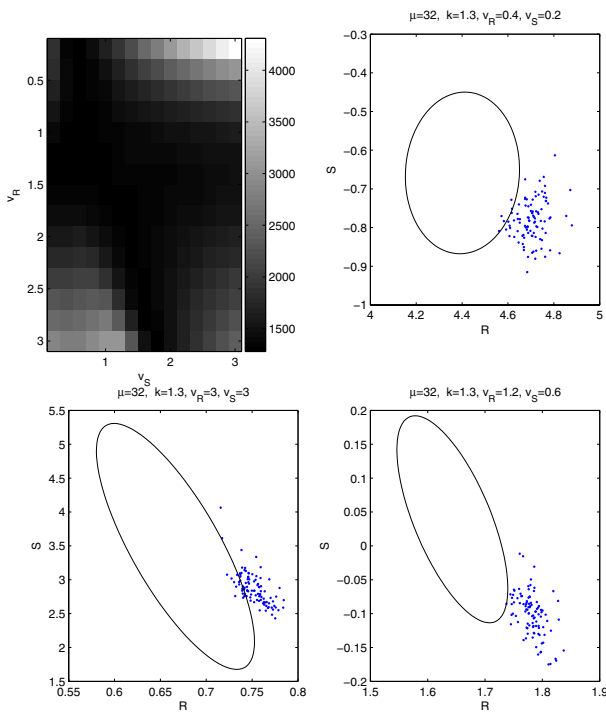


Fig. 5. Top left: summation of  $p_{FDS}$  over the area *C* in Figure 4 as a function of  $v_R$  and  $v_S$ . The bigger number indicates bigger false acceptance and therefore should be avoided. Top right and bottom left and right: The  $R - S$  values of 100 sets of coherent data (each set has 5000 sample data *A*) for different  $v_R$  and  $v_S$  values as labelled. A more reliable discriminant function will classify less percentage of the points as *FDS* (bottom right).

### B. Minimizing False Acceptance for Few Scatterer Sets

We sum  $p_{FDS}$  over the area *FS* in Figure 4 to minimize false acceptance of the sets with low scatterers (Figure 6 top left). The low values for  $v_R$  and  $v_S$  suffer from high false acceptance (Figure 6 top right and bottom left). A  $v_R > 2$

and  $v_S < 1.5$  value generates low false acceptance (Figure 6 bottom right).

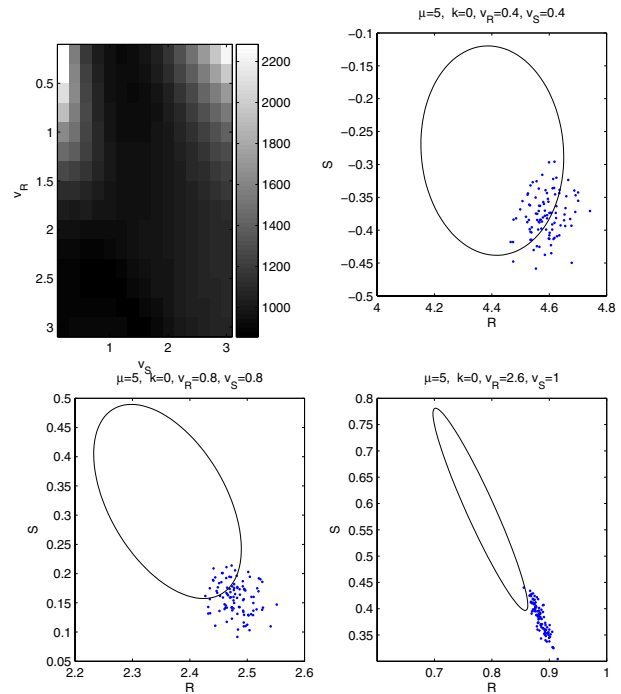


Fig. 6. Top left: summation of  $p_{FDS}$  over the area *FS* in Figure 4 as a function of  $v_R$  and  $v_S$ . The bigger number indicates bigger false acceptance and therefore should be avoided. Top right and bottom left and right: The  $R - S$  values of 100 sets of few scatterers data (each set has 5000 sample data *A*) for different  $v_R$  and  $v_S$  values as labelled. A more reliable discriminant function will classify less percentage of the points as *FDS* (bottom right).

### C. Minimizing False Rejection for *FDS* Sets

To minimize the rejection of *FDS* sets, we sum  $p_{FDS}$  over the area *FDS* in Figure 4. Figure 7 shows the results.

## IV. EXPERIMENTAL RESULTS

Based on the results of Figures 5 and 6, we conclude that in order to minimize false acceptance of non-*FDS* sets  $v_S$  has to be approximately half of  $v_R$ . We performed the  $R - S$  speckle detection method with different  $v_R$  and  $v_S$  values on bovine liver B-scans.

Figure 8 shows the image divided into patches of  $100 \times 50$  pixels. The  $R$  and  $S$  values of each patch is calculated. The resultant point in the  $R - S$  plane is connected to the center of the *FDS* discriminant ellipse and the ratio of the length of the line segment to the radius of ellipse at the intersection of the line segment and the ellipse is shown at the center of each patch. A patch with the ratio less than 1 can be considered as a *FDS* patch.

While the three different  $v_R$  and  $v_S$  values give similar results for the patches that are close to *FDS*, the pair  $v_R = 2$  and  $v_S = 1$  yields larger values for patches that are clearly not *FDS* (some samples marked by circle).

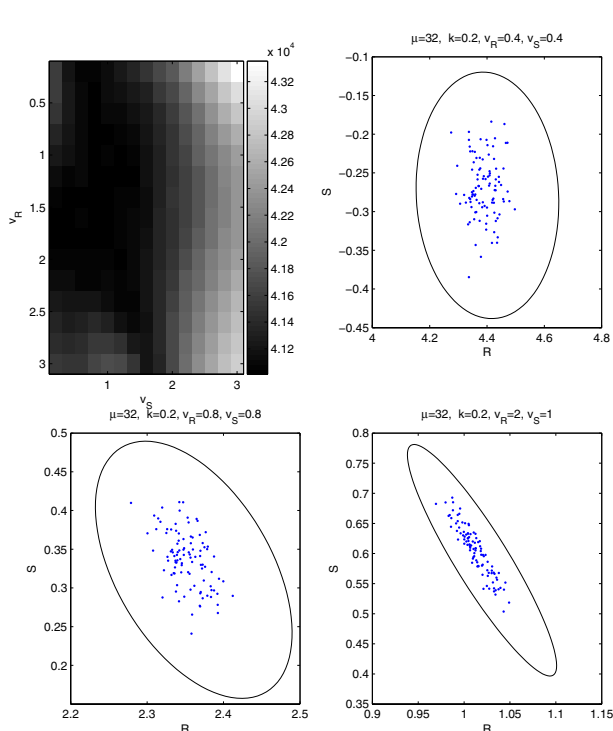


Fig. 7. Top left: summation of  $p_{FDS}$  over the area  $FDS$  in Figure 4. The bigger number indicates better acceptance of the FDS. Top right and bottom left and right: The  $R - S$  values of 100 sets of FDS data (each set has 5000 sample data  $A$ ) for different  $v_R$  and  $v_S$  values as labelled. All three cases perform well in accepting FDS.

## V. DISCUSSION AND CONCLUSION

This work provides a complete simulation analysis for finding optimum powers to classify speckles. In ultrasound images, one patch includes a variety of backscattering effects: FDS, few scatterers and coherent scatterers. A future research direction would be to consider sets that have a mixture of samples with different  $\mu$  and  $k$  values. This is, however, challenging since the percentage of each set should be relevant to what is observed in real tissue. Therefore the sensitivity of the results to the percentages of data with specific  $\mu$  and  $k$  value should be considered. The attenuation effect is not also considered in this work, which is specifically important for patches that are elongated in the axial direction.

To achieve optimal results in the moment-based speckle classification method discussed in this work, the sample power in  $S$  has to be approximately half of the sample power in  $R$ . The values for  $v_R$  and  $v_S$  have to be selected according to specific concerns: minimizing false acceptance or false rejection or a combination of both. The three optimization criteria analyzed in this work provide a guideline for choosing appropriate values. Proper power selection can result in 50% more reliable classification.

### ACKNOWLEDGMENT

Funded by NSF ERC #EEC 9731478. Authors acknowledge Siemens Corporate Research and Ultrasound Department.

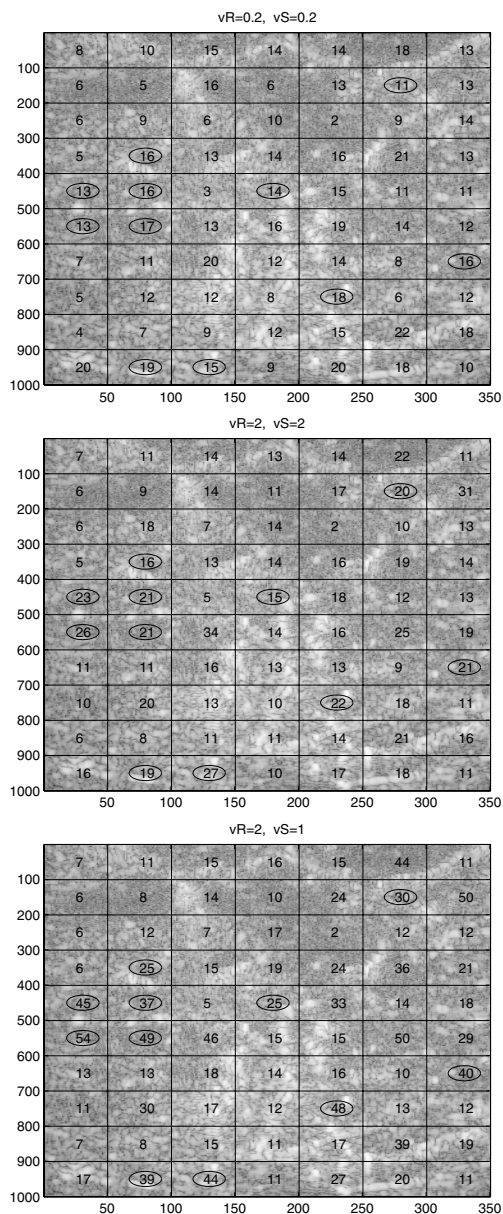


Fig. 8. Bovine liver B-scans at three different  $v_R$  and  $v_S$  values as labelled (specular top and noisy bottom are discarded). The numbers at the center of each patch indicates how close the  $R$  and  $S$  of the patch is to the FDS ellipse. Big numbers are assigned to the patches that clearly are not FDS (marked by a circle around the number) in the bottom image.

### REFERENCES

- [1] R. Prager, A. Gee, G. Treece, and L. Berman, "Analysis of speckle in ultrasound images using fractional order statistics and the homodyned  $k$ -distribution," *Ultrasonics*, vol. 40, pp. 133–137, 2002.
- [2] M. Martin-Fernandez and C. Alberola-Lopez, "On low order moments of the homodyned- $k$  distribution," *Ultrasonics*, vol. 43, pp. 283–290, 2005.
- [3] V. Dutt and J. Greanleaf, "Ultrasound echo envelope analysis using a homodyned  $k$  distribution signal model," *Ultrasonic Imaging*, vol. 16, pp. 265–287, 1994.
- [4] V. Dutt and J. Greanleaf, "Speckle analysis using signal to noise ratios based on fractional order moments," *Ultrasonic Imaging*, vol. 17, pp. 251–268, 1995.